

Medical Image Classification Using RNN in Quadri-Partitioned Neutrosophic Set

A. Panimalar , D. Aarthi , S. Santhosh Kumar

Sri Ramakrishna Mission Vidyalaya College of Arts and Science, Coimbatore, India.

Abstract:-The classification of brain tumor is essential for both diagnostic and therapeutic planning. Recurrent neural networks (RNNs) have demonstrated promising results in analyzing sequential data in recent years. Quadri-partitioned neutrosophic sets additionally offer a structure for capturing ambiguities and uncertainties in classification problems. This study investigates the categorization of brain tumors using an RNN with a quadri-partitioned neutrosophic set. The study aims to increase classification accuracy and offer information on how certain forecasts can be made. The suggested method QPN-RNN's accuracy in classifying brain tumors while considering the quadri-partitioned neutrosophic set is shown by experimental data.

Keywords: *Quadri-partitioned neutrosophic set, Recurrent neural network.*

1.Introduction

A new topic of study in the realm of machine learning and medical image analysis is the categorization of brain tumors using recurrent neural networks (RNNs) and medical images. The ability to analyse sequences of data makes RNNs an excellent choice for applications involving sequential data, such as time series or the spatial information present in medical images. A unique structure called a recurrent neural network (RNN) [1] seeks to utilise the temporal information of the input data. RNN is created because MLP suffers from neglecting the connections between the present input data and the previous and subsequent input data. RNN can transmit temporal information over the network, as opposed to MLP. It is crucial to time series analysis, including recognition of speech [2], emotion classification [3], and machine translation [4].

The classification of brain tumors is essential for detecting and managing disorders affecting the brain. Traditional image classification techniques frequently miss the uncertainties included in medical images, resulting in incorrect classifications. The traditional classification approaches often overlook the inherent uncertainties and ambiguities associated with predictions[16]. To address this limitation, quadri-partitioned neutrosophic sets provide a valuable framework. By considering the four partitions of true positive (TP), true negative (TN), false positive (FP), and false negative (FN), quadri-partitioned neutrosophic sets (QNS) allow for a more nuanced analysis of classification outcomes.

In this paper it is suggested to use a quadri-partitioned neutrosophic set, which offers a more thorough representation by taking into account the positive, negative, contradictory, and ignorant characteristics of tumor regions, to solve this problem. This uses recurrent neural networks (RNNs) to their full potential to efficiently simulate the temporal dependencies found in sequential medical data, such as images of brain tumors. Incorporating the quadri-partitioned neutrosophic set into the RNN architecture enhances the precision and robustness of brain tumor classification.

In order to classify brain tumours, this study suggests combining an RNN model with a quadri-partitioned neutrosophic set. The quadri-partitioned neutrosophic set adds some ambiguity and uncertainty to the predictions while the RNN captures the temporal relationships in the tumour image sequences. The model can produce more accurate and illuminating categorization results by taking into account the membership degrees assigned to each partition.

Here, the basic definitions and concepts of the quadri-partitioned Neutrosophic set are given in Section 2. In Section 3, the formulas are given for converting a spatial domain image into a quadri-partitioned neutrosophic domain. In Section 4, Proposed proposed quadri-partitioned neutrosophic RNN (QPN-RNN) algorithm is given step by step. RNN architecture and recurrent neural network (RNN) design were explained in detail in sections 5 and 6, respectively. In Section 7, details of the data set that is used for this proposed work were given. In Section 8, Results and Discussion were explained. Finally, in Section 9, the proposed work conclusion was given.

2. Quadri-Partitioned Neutrosophic set

In 1965, Zadeh [7] introduced the fuzzy set. F. Smarandache proposed the idea of a Neutrosophic set, that is a mathematical technique for dealing with issues including imperfect, ambiguous, and inconsistent data. In the suggested neutrosophic sets, Smarandache [8]. The uncertainty membership function in neutrosophic sets moves independently of membership in truth or falsehood. Researchers have thoroughly studied the neutrosophic theory for use in handling ambiguous real-world circumstances. Although the neutrosophic theory's hesitation margin is unaffected by truth or falsity membership, it now appears to be more comprehensive than intuitionistic fuzzy sets. In a recent study by Atanassov et al. [9], the relationships between inconsistent intuitionistic fuzzy sets, picture fuzzy sets, neutrosophic sets, and intuitionistic fuzzy sets were explored. However, an unresolved question remains: whether the uncertainty associated with a specific element is due to its belongingness or non-belongingness. Chatterjee et al. [10] brought attention to this issue while introducing a more comprehensive structure of neutrosophic sets known as the quadripartitioned single-valued neutrosophic set (QSVNS).

The concept of QSVNS is derived from Smarandache's four numerical-valued neutrosophic logic and Belnap's four-valued logic. In this framework, uncertainty is divided into two distinct parts: "ignorance," representing neither true nor false, and "contradiction," indicating that the element is both true and false simultaneously. In the context of neutrosophic studies, the QSVNS appears to be a logical extension. Furthermore, Chatterjee et al. [4] analyzed a real-life example to offer a deeper understanding of the QSVNS environment, demonstrating that such situations naturally occur. The Quadri – partitioned neutrosophic set is defined as follows: [11]

Definition:1(Quadri – Partitioned Neutrosophic Set)

Let X be a universe set. A Quadri-Partitioned Neutrosophic set N with independent neutrosophic components on X is an object of the form $N = \{ \langle x, T_N(x), C_N(x), U_N(x), F_N(x) \rangle : x \in X \}$ and $0 \leq T_N(x) + C_N(x) + U_N(x) + F_N(x) \leq 4$. Here, $T_N(x)$ is the truth membership, $C_N(x)$ is contradiction membership, $U_N(x)$ is ignorance membership and $F_N(x)$ is the false membership.

3. Converting Spatial domain image into Quadri-Partitioned Neutrosophic domain:

The following formulae are used to convert the spatial domain image into a quadri-Partitioned Neutrosophic domain: [12][13][14]

$$T(a, b) = \frac{\bar{A}(a, b) - \bar{A}_{\min}}{\bar{A}_{\max} - \bar{A}_{\min}} \quad (1)$$

Where $\bar{A}(a, b)$ is the local mean value of the pixel of the image.

$$\bar{A}_{\max} = \max \bar{A}(a, b) \quad (2)$$

$$\bar{A}_{\min} = \min \bar{A}(a, b) \quad (3)$$

$$\bar{A}(a, b) = \frac{1}{w \times w} \sum_{i=a-\frac{n}{2}}^{a+\frac{n}{2}} \sum_{j=b-\frac{n}{2}}^{b+\frac{n}{2}} A(i, j) \quad (4)$$

$$U(a, b) = \frac{g(a, b) - g_{\min}}{g_{\max} - g_{\min}} \quad (5)$$

(a, b) is the absolute value of difference between intensity $A(a, b)$ and its local mean value $\bar{A}(a, b)$.

$$g(a, b) = \text{abs}(g(a, b) - \bar{g}(a, b)) \quad (6)$$

$$g_{\max} = \max g(a, b) \quad (7)$$

$$g_{\min} = \min g(a, b) \quad (8)$$

$$C(a, b) = 1 - U(a, b) \quad (9)$$

$$F(a, b) = 1 - T(a, b) \quad (10)$$

3.1 Definition of TP, TN, FP, FN for QNS:

TP-QNS (True set (T)): TP-QNS (True positives) equation (1) are QNSs that show a high truth membership and a low falsity membership when both the ground truth and forecasted QNSs show the same. In other words, there is great confidence in the agreement between the prediction and the ground truth regarding the positive class.

TN-QNS (False set (F)): TN-QNS (True Negatives) equation (10) are QNSs that show a high falsity-membership and a low truth-membership in both the ground truth and anticipated QNSs. In other words, there is great confidence in the agreement between the prediction and the ground truth regarding the negative class.

FP-QNS (Contradiction(C)) : FP-QNS (False positives) equation (9) are when the anticipated QNS has a high truth membership but the ground truth QNS shows a high falsity membership. In other words, the ground truth strongly suggests a negative class, whereas the forecast strongly suggests a positive class.

FN-QNS (Ignorance set (U)) : FN-QNS (False negatives) equation (5) are when the anticipated QNS shows a high falsity membership while the ground truth QNS shows a high truth membership. In other words, the ground truth strongly suggests a positive class, whereas the forecast strongly suggests a negative class.

4. ProposedQuadri-Partitioned Neutrosophic RNN (QPN-RNN) Algorithm

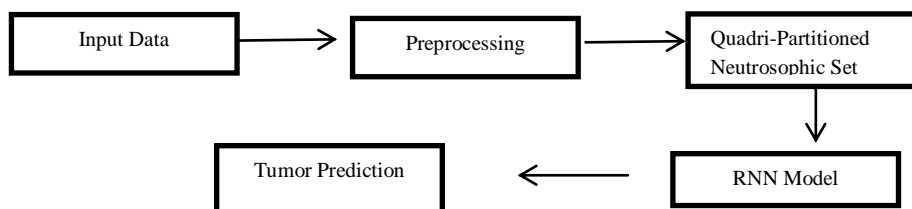


Fig 1 :Flow chart for QPN-RNN

Step:1. Load and preprocess the brain tumor dataset.

Step:2. Split the dataset into training and testing sets.

Step:3. Define the quadri-partitioned neutrosophic set with four partitions: TP, TN, FP and FN.

Step:4. Initialize the RNN architecture.

Step:5. Set the loss function and optimizer for the model.

Step:6. Train the model using the training dataset.

6.1. Iterate through the training data in mini-batches.

6.2. Forward propagate the input through the RNN layers.

6.3. Calculate the loss between the predicted and actual labels.

6.4. Back propagate the loss and update the model's parameters.

6.5. Repeat steps 6.1-6.4 until all training data is processed.

Step:7. Evaluate the model using the testing dataset.

7.1. Iterate through the testing data.

7.2. Forward propagate the input through the RNN layers.

7.3. Calculate the quadri-partitioned neutrosophic set for each prediction.

7.4. Compare the predicted labels with the actual labels and calculate evaluation metrics

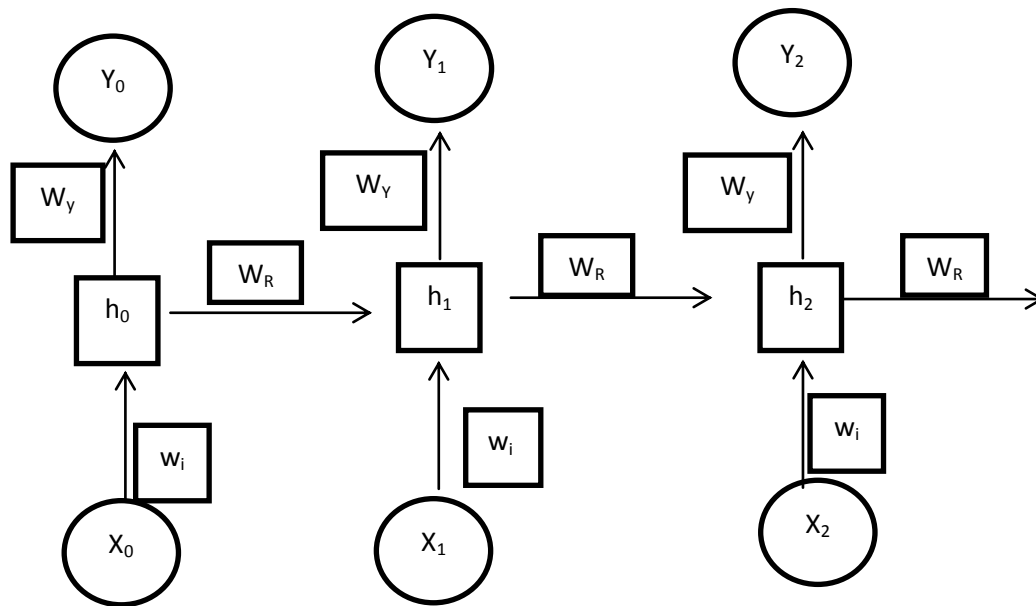


Fig 2 :RNN architecture

5.RNN architecture

The algorithm of the RNN is here taken x as input at the given time t . Next, the current hidden state h at time t will be calculated as follows:

$$h^{(t)} = G_h(W_i x^{(t)} + W_R h^{(t-1)} + b_h) \quad (11)$$

where $h^{(t)}$ represents the state of the hidden unit, W_i represents the weight used for hidden state computation, W_y represents the weight for output computation and W_R represents the weight for hidden state computation from the previous hidden state. Finally, the current output at time t will be computed using the following formula:

$$y^{(t-1)} = G_y(W_y h^{(t)} + b_y) \quad (12)$$

$y^{(t-1)}$ represents the state of the output. b_n , b_y are, represents the bias in the neural network.

6. Recurrent neural network (RNN)

Each element has a particular function in the network design of an RNN, starting with convolutional layers, batch normalisation, ReLU activation, and max pooling, followed by sequence folding layers, LSTM layers, a fully connected layer, a softmax layer, and a classification layer. Begin to examine each component's function and training:

6.1 Convolutional layers

The convolution layer used to extract features from the input images, the layers are frequently utilised in tasks involving images. The input is subjected to a set of learnable filters by these layers, which organise over the image to generate feature maps. The Gradient descent optimisation techniques, here Adam in this instance, and back propagation are used to learn the convolutional filter weights (parameters) during training. For stabilise and speed up the training process, the batch normalisation layer normalises the convolutional layer's output.

6.2. ReLU activation

The activation function of the ReLU (Rectified Linear Unit) brings nonlinearity into the network [15]. It applies an element-by-element activation, maintaining positive values while setting negative values to zero. ReLU enhances the network's capacity to simulate nonlinear interactions and aids in the network's ability to learn complex representations.

6.3. Max Pooling

Max pooling minimises the feature maps' spatial dimensions while keeping the standout features. It chooses the highest value possible inside each zone after dividing the feature map into non-overlapping regions. The feature maps can be downscaled using max pooling, which lowers the number of parameters and simplifies the computation[5].

6.4. Sequence folding layer

Convolutional layers' spatial data are transformed into a sequence format by the sequence folding layer so that the LSTM layers can handle it. It maintains the order of occurrence of the input while converting the 3D feature maps into a 2D sequence of vectors.

6.5. LSTM layers

LSTM layers, a subset of recurrent layers, are capable of detecting long-distance dependencies and sequential patterns in data. They are made up of memory cells that enable long-term information storage and retrieval. Back propagation through time (BPTT), which applies back propagation to recurrent connections, is used to train LSTM layers. Based on the input sequences, hidden states, and cell states, the LSTM layers gradually learn to update and forget information[6]. Here 64 and 32 hidden units in the LSTM layers, respectively, are numerous and help in learning various facets of the data.

6.6. Fully Connected Layer

The information from the LSTM layers is combined and mapped to the desired output size by the fully connected layer. It does a linear transformation, then an activation function, which results in the output being non-linear. Here, 2 neurons in a fully linked layer for binary classification (brain tumour or not).

6.7. Softmax Layer

The output of the previous layer is transformed into a probability distribution over the classes by the softmax layer. It assigns a probability to each class that reflects the degree of confidence the network has in the prediction.

6.8. Classification Layer

The probabilities provided by the softmax layer are used by the classification layer to assign a class label. Using gradient descent and back propagation, the fully connected layer, softmax layer, and classification layer parameters are learned during training. And enhance the performance of the network, the loss between the predicted probabilities and the ground truth labels is minimized.

The network is trained using the training parameters that have been set, including the Adam optimizer, learning rate, number of epochs, mini-batch size, and validation frequency. Iteratively feeding training data into the network, computing loss, and updating weights using gradients obtained from back propagation are all steps in the training process. The network's capability to produce accurate predictions on the brain tumor dataset gradually gets better as a result of this process, which lasts for the designated number of epochs.

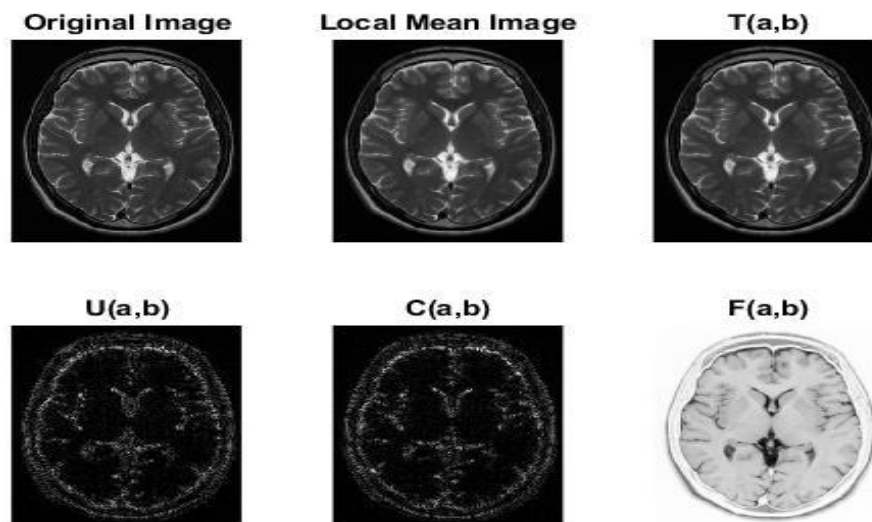


Fig 3 :Quadri-partitioned Neutrosophic output images

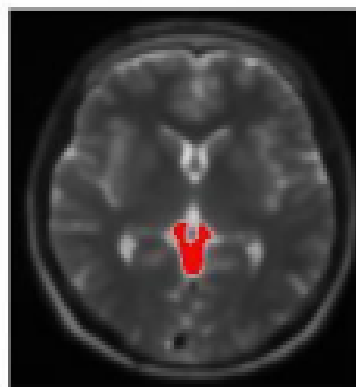


Fig 4 :QPN-RNN method tumor image

7. Details of Data set:

The Kaggle database is where the information is found. 3264 data details are provided. A range of brain tumour MRIs, including gliomas, meningiomas, no tumours, and pituitary tumours, are included in the database. Here, 750 training data and 500 testing data are gathered.

8. Results and Discussion

8.1. Evaluation Metrics

The confusion matrix, which breaks down the model's predictions into true positives, true negatives, false positives, and false negatives, should be calculated and examined. The quadri-partitioned neutrosophic set evaluation makes use of this matrix particularly well.

TP 396	FP 6
FN 4	TN 94

Fig5 :Confusion Matrix

Using the procedures of accuracy, dice, sensitivity, specificity, and jaccard, the performance is calculated. Sensitivity (also known as the true positive fraction or recall) is the proportion of real positives that are anticipated to be positive. Defined mathematically as

$$\text{Sensitivity} = \frac{TP}{TP+FN} = 99\%$$

$$\text{Specificity} = \frac{TN}{TN+FP} = 94\%$$

$$\text{Accuracy} = \frac{TP+TN}{TP+TN+FP+FN} = 98\%$$

$$\text{Dice} = \frac{2TP}{(TP+FP)+(TP+FN)} = 98.7\%$$

$$\text{Jaccard} = \frac{TP}{TP+FP+FN} = 97.5\%$$

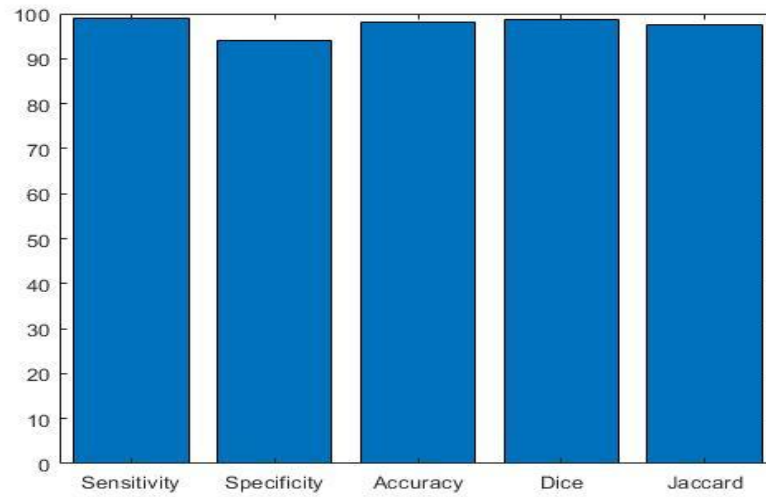


Fig 6 :Performance Evaluation graph

Table 1: Accuracy percentage of brain tumor detection

S.No.	Number of MRI Brain samples	Accuracy Percentage of brain tumor detection
1	50	98.65
2	100	98.53
3	150	98.41
4	200	98.86
5	250	98.73
6	300	97.96
7	350	97.89
8	400	97.77
9	450	96.93
10	500	96.84

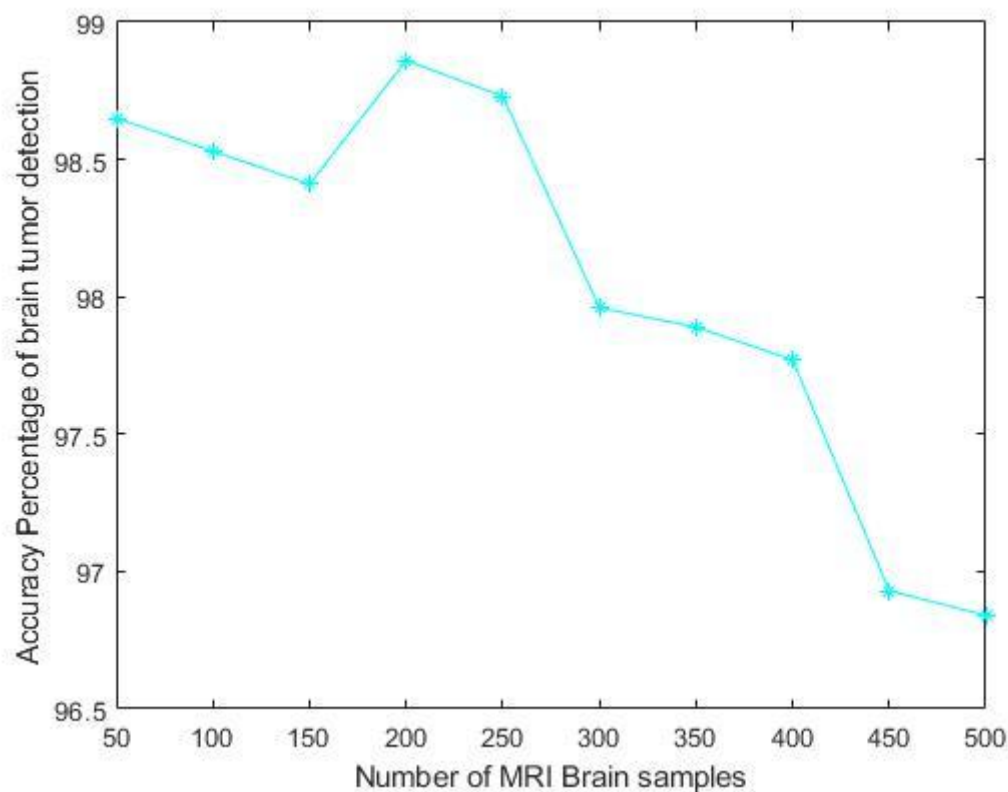


Fig 7 :Graph of Accuracy percentage of brain tumor detection

The experimental results demonstrate that the proposed QPN-RNN model in the quadripartitionedneutrosophic set achieves average accuracy 98.05% of superior performance in brain tumor image classification compared to traditional methods. The quadripartitionedneutrosophic set provides a more comprehensive representation, effectively capturing the uncertainties inherent in medical images. The QPN-RNN architecture effectively models the temporal dependencies, leading to improved accuracy and robustness in classification. Furthermore, the approach shows promising potential in handling complex and dynamic tumor patterns.

9. Conclusion

In this study, we presented a novel approach for brain tumor image classification using an RNN in the quadripartitioned neutrosophic set. Our results highlight the effectiveness of this approach in accurately classifying brain tumor images while considering uncertainties. The quadripartitionedneutrosophic set enables a more comprehensive representation of tumor regions, leading to improved classification performance. The QPN-RNN architecture successfully captures temporal dependencies, enhancing the model's ability to recognize complex tumor patterns. This work contributes to the advancement of brain tumor classification and paves the way for future research in utilizing the quadripartitionedneutrosophic set and RNNs for medical image analysis and diagnosis.

Reference

- [1] Chao Yang, Wenxiang Jiang, & Zhongwen Guo. (2019). Time Series Data Classification Based on Dual Path CNN-RNN Cascade Network, IEEE, 7. doi:10.1109/access.2019.2949287 .
- [2] Graves, A., Mohamed, A.R., & Hinton, G. (2013). Speech recognition with deep recurrent neural networks, in Proc. IEEE Int. Conf. Acoust., Speech Signal Process, pp.6645–6649. <https://ieeexplore.ieee.org/document/6638947>.
- [3] [Rana, R. (2016). Gated recurrent unit (GRU) for emotion classification from noisy speech.

-
- arXiv:1612.07778. [Online]. Available: <https://doi.org/10.48550/arXiv.1612.07778>.
- [4] Bahdanau, D., Cho, K., & Bengio, Y. (2014). Neural machine translation by jointly learning to align and translate. arXiv:1409.0473. [Online]. Available: <https://arxiv.org/abs/1409.0473>.
 - [5] Haoming Li, Jinghui Fang, et al. "CR-Unet: A Composite Network for Ovary and Follicle Segmentation in Ultrasound Images". Journal of Biomedical and Health Informatics, IEEE. 1-1. (2019). doi:10.1109/JBHI.2019.2946092.
 - [6] Yann LeCun, Yoshua Bengio & Geoffrey Hinton. (2015) *Deep learning*, Nature, 521(7553), 436–
 - [7] 444. doi:10.1038/nature14539. Zadeh, L. A. Fuzzy Sets. (1965) Inform and Control 8, 338 – 353. [https://doi.org/10.1016/S0019-9958\(65\)90241](https://doi.org/10.1016/S0019-9958(65)90241).
 - [8] Smarandache, F. (2002). Neutrosophy and Neutrosophic Logic. First International Conference on Neutrosophy, Neutrosophic Logic, Set, Probability and Statistics. University of New Mexico, Gallup, NM 87301, USA. <https://arxiv.org/ftp/math/papers/0306/0306384.pdf>.
 - [9] Atanassov, K. (1986). Intuitionistic fuzzy sets. Fuzzy Sets and Systems, 20(1). pp. 87-96 [https://doi.org/10.1016/S0165-0114\(86\)80034-3](https://doi.org/10.1016/S0165-0114(86)80034-3).
 - [10] Chahhterjee, R., Majumdar, P., & Samanta, S. K. (2016). On some similarity measure and entropy on Quadripartitioned single valued neutrosophic sets. Journal of Intelligent & Fuzzy Systems 30, 2475–2485 doi:10.3233/IFS-152017.
 - [11] Radha, R., Stanis Arul Mary, A. (2020). Quadri Partitioned Neutrosophic Pythagorean Set. International Journal of Research Publication and Reviews .2 (4) .pp. 276-281. <https://fs.unm.edu/neut/QuadriPartitionedNeutroPythagorean.pdf>.
 - [12] Mohan, J., Thilaga Shri Chandra, A. P., Krishnaveni, V., Yanhui Guo, (2012). Evaluation of Neutrosophic set approach filtering technique for image denoising. IJMA, 4(4). doi: [10.5121/ijma.2012.4407](https://doi.org/10.5121/ijma.2012.4407).
 - [13] Radha, R., Stanis Arul Mary, A. (2021). Pentapartitioned Neutrosophic Pythagorean Set. International Research Journal on Advanced Science Hub (IRJASH). 3 (2). https://rspsciencehub.com/article_8441_91a20a850d986b064e3632037146114a.pdf.
 - [14] Rajashi Chatterjee, Majumdar, P. & Samanta, S. K. (2016) On some similarity measures and entropy on quadripartitioned single valued neutrosophic sets. Journal of Intelligent & Fuzzy Systems 30, pp. 2475–2485, doi:10.3233/IFS-152017
 - [15] Lichao Mou, Pedram Ghamis & Xiao Xiang Zhu. (2017). Deep Recurrent Neural Networks for Hyperspectral Image Classification. IEEE Transactions on geoscience and remote sensing, pp. 1–17. doi:10.1109/TGRS.2016.2636241.
 - [16] Varalakshmi, A., Kumar, S. S., Shanmugapriya, M. M., Mohanapriya, G., Anand, M., C., J. (2022). Markers
 - [17] location Monitoring on images from an infrared camera using optimal fuzzy inference system. International Journal of Fuzzy Systems. <https://link.springer.com/article/10.1007/s40815-022-01407-8>.